



Published in final edited form as:

*Laryngoscope*. 2016 March ; 126(3): 657–664. doi:10.1002/lary.25506.

## A Multi-Sensor Approach to Improve Manometric Analysis of the Upper Esophageal Sphincter

Corinne A Jones, MS<sup>1,2,3</sup>, Michelle R Ciucci, PhD<sup>1,2,3</sup>, Michael J Hammer, PhD<sup>1</sup>, and Timothy M McCulloch, MD<sup>1,2</sup>

<sup>1</sup>Department of Surgery, Division of Otolaryngology, University of Wisconsin-Madison, Madison, WI, USA

<sup>2</sup>Department of Communication Sciences and Disorders, University of Wisconsin-Madison, Madison, WI, USA

<sup>3</sup>Neuroscience Training Program, University of Wisconsin-Madison, Madison, WI, USA

### Abstract

**OBJECTIVES/HYPOTHESIS**—High-resolution manometry (HRM) improves on previous manometric systems by including a greater number of sensors that are more densely-placed. Due to deglutitive movement of the HRM catheter and UES, it is unclear which HRM sensors capture pressure in the upper esophageal sphincter (UES). To address this issue, we present two complementary studies to describe UES pressure patterns using HRM+videofluoroscopy and HRM+electromyography (EMG).

**STUDY DESIGN**—Case series involving new analysis method.

**METHODS**—*Study 1*: Simultaneous HRM+videofluoroscopy were performed in 11 healthy subjects swallowing five 10mL thin-liquid boluses. HRM catheter and UES movement were tracked to identify UES pressure patterns over multiple HRM sensors. *Study 2*: Simultaneous HRM+cricopharyngeal-EMG were performed in 6 healthy subjects swallowing five 10mL water boluses. HRM and EMG outputs were correlated over individual and multiple HRM sensors.

**RESULTS**—HRM sensors move prior to UES movement ( $p < 0.001$ ) and to a lesser extent in rostral and ventral directions ( $p = 0.01$ ) than the UES. UES closing pressure is captured with two distinct patterns: 1) a rostral-UES pattern with short durations and fast rate of pressure release, depicting UES descent along the catheter as it closes; and 2) a caudal-UES pattern with tonic pressures at baseline and a deglutitive nadir. The HRM+EMG multi-sensor correlation ( $r = 0.88$ ) was significantly stronger than the single-sensor correlation ( $r = 0.80$ ;  $p = 0.02$ ).

---

Corresponding author: Timothy M. McCulloch, M.D., Address: Box 7375 Clinical Science Center – H4, 600 Highland Ave, Madison, WI 53792, Telephone number: 608-263-0192, Fax number: 608-252-0925, mccull@surgery.wisc.edu.  
Institution: University of Wisconsin-Madison

Conflict of interest: The authors have no conflicts of interest to declare.

Parts of this manuscript were presented at the Dysphagia Research Society Meeting on March 10, 2012 (Toronto, ON, CA) and on March 15, 2013 (Seattle, WA, USA).

**CONCLUSION**—During deglutition, the HRM catheter and the UES rise above baseline positions and create a distinctive, multi-sensor manometric trace. Accurate deglutitive UES pressure evaluation must include multiple manometric sensors.

### Keywords

Deglutition; Upper Esophageal Sphincter; High-Resolution Manometry; Videofluoroscopy; Electromyography

---

## INTRODUCTION

The upper esophageal sphincter (UES) is a region of high pressure at the pharyngo-esophageal junction. The UES encompasses the cricopharyngeus (CP), inferior pharyngeal constrictor, and rostral esophageal musculature<sup>1-4</sup>. During swallowing, the UES opens via cricopharyngeal relaxation<sup>1,5,6</sup>, anterior hyolaryngeal complex movement due to suprahyoid muscular contraction<sup>1,7,8</sup>, and distension secondary to intrabolus pressure<sup>8-10</sup>. UES-related dysphagia can therefore be caused by abnormal relaxation of the cricopharyngeus, inadequate hyolaryngeal excursion, reduced oropharyngeal motility, or structural noncompliance of UES musculature<sup>11</sup>. Consequences of UES-related dysphagia include bolus residual in the pharynx, airway invasion, and swallowing inefficiency<sup>12-14</sup>. Due to the multiple causes of deglutitive UES opening, integrative evaluations of UES function are necessary to determine underlying causes of UES dysfunction and plan appropriate treatment: 1) electromyography (EMG) to measure contractile properties of UES and suprahyoid musculature; 2) visualization techniques, e.g., videofluoroscopy, to measure UES patency and pharyngeal kinematics; and 3) manometry to measure intrabolus pressure and pressure-related outcomes of muscular contraction and relaxation<sup>1,2,4,7,15,16</sup>. These methods are not without limitations: 1) intramuscular EMG is invasive and limited to use by trained physicians; 2) videofluoroscopy involves radiation exposure and has limited temporal resolution; and 3) manometry analysis can be difficult and has been limited by sensors density in the pharynx.

Manometry is useful for assessing UES function, as it is available to a wide range of health professionals<sup>17,18</sup> and provides objective information regarding static pressure and pressure changes during UES relaxation and contraction. High-resolution manometry (HRM) improved upon limitations of conventional manometry by including up to 36 circumferential pressure sensors at ~1cm intervals. This increases fidelity of pressure information compared to older techniques, which used fewer, more sparsely-spaced sensors with unilateral data-collection<sup>1,2,5,7-9,16</sup>. Due to the close proximity of HRM sensors, pressure information is recorded on adjacent sensors; pressure data is captured from mobile pharyngeal structures, such as the shortening pharynx and elevating UES<sup>7,10,19,20</sup>. Thus, HRM is essential for accurate evaluation of deglutitive UES pressures.

Although HRM can capture relevant pressure data, analysis of UES pressure is complicated by deglutitive movement of the manometric catheter and UES high-pressure zone. During swallowing, velopharyngeal port closure results in ~1.0cm of rostral catheter movement<sup>7,19</sup>. The UES independently rises between 2.0–2.8cm<sup>7,19,20</sup>, due to hyolaryngeal complex

excursion<sup>8</sup> and pharyngeal shortening<sup>20,21</sup>. Kahrilas and colleagues<sup>7</sup> described that, after bolus passage, the UES begins to close at a point above its baseline position. While closing and descending UES pressures can be measured over multiple HRM sensors, the standard spatio-temporal plot infers static positions of both sensors and pharyngeal structures, potentially confounding interpretation of pharyngeal and UES pressure events (Figure 1). Currently, there is no consensus on how to track these movements on HRM output.

Some reports of UES pressure amplitudes and durations use eSleeve functionality included with HRM systems<sup>22,23</sup>. eSleeve algorithms were designed for detecting lower esophageal sphincter movement and display the highest pressure over 4–6 sensors<sup>24,25</sup>. To the authors' knowledge, no validation studies have been completed to justify use of eSleeve algorithms in the UES. Additionally, Ghosh and colleagues<sup>10</sup> described methods to calculate pressures associated with UES movement. However, these require exporting data into a separate program and interpolating data using multiple algorithms. This technique fails to utilize pressure information provided by commercially-available HRM systems. There is a need for a simple, valid method to determine which HRM sensors display deglutitive UES pressure.

The purpose of these studies was to classify manometric patterns relating to deglutitive UES and catheter movement and to verify UES pressure patterns with cricopharyngeal-EMG activity. We present two complementary studies: 1) HRM+videofluoroscopy to analyze pressure patterns based on relative UES and manometric sensor location; and 2) HRM+cricopharyngeal-EMG to analyze muscular contributions to deglutitive UES pressures over multiple HRM sensors. We hypothesized that: 1) during swallowing, UES movement produces a visually-distinct pressure pattern discernible from pressure sources elsewhere in the pharyngo-esophagus; 2) deglutitive UES movement will be supported by correlations between deglutitive UES pressure and cricopharyngeal-EMG activity; and 3) correlations will be strongest when incorporating multiple manometric signals.

## STUDY 1: HRM+VF

### MATERIALS AND METHODS

**Equipment**—High-Resolution Manometry: UES pressure was recorded with solid-state high-resolution manometry (ManoScan<sup>360</sup>, Given Imaging, Atlanta, GA). The manometric catheter has an outer diameter of 2.75mm and is comprised of 36 pressure sensors, spaced 1cm apart. Each sensor receives input from 12 circumferential elements, which the system averages to one signal. The system records pressure between –20 and 600 mmHg, with fidelity of 2mmHg and at a sampling rate of 50Hz (ManoScan Data Acquisition, Given Imaging). The catheter was calibrated before use according to manufacturer specifications.

**Videofluoroscopy**: Continuous videofluoroscopy was performed in the lateral plane (OEC 9900, General Electric, Fairfield, CT). Video was recorded to DVD (DVO-1000MD, Sony, Park Ridge, NJ) at 30 frames/second. Boundaries included the incisors, cervical vertebrae, nasal border of the soft palate, and cervical esophagus.

**Participants**—Eleven adults (4 males) participated with informed consent and under approval from the University of Wisconsin-Madison Institutional Review Board. The board

approved the use of videofluoroscopy in healthy individuals with the appropriate statement of risk vs. benefit in the consent form. Participants were of a mean age of 33 years (range: 21–52) and had no history of swallowing, gastrointestinal, or neurologic disorders.

**Procedure**—Participants sat upright for the entire procedure. The nasal passage was anesthetized with <0.5mL topical 2% viscous lidocaine hydrochloride. Catheter placement was standardized such that each pharyngeal region of interest was captured, as described in McCulloch, et al.<sup>26</sup> Participants rested for 5 minutes to adjust to the catheter before performing experimental swallows. Participants swallowed five 10mL boluses of thin-liquid barium at a 40% weight-to-volume ratio (Varibar, Monroe Township, NJ) with the head in a neutral position. Participants waited to swallow until cued by the experimenter.

**Data Analysis**—Manometric and videofluoroscopic data were time-aligned with a timecode embedded into the videofluoroscopy signal (UTG-50, Horita, Mission Viejo, CA). Videofluoroscopic images were imported into ImageJ (National Institutes of Health, Bethesda, MD) and rotated such that a line connecting anterior-inferior corners of C2 and C4 vertebrae was parallel to the y-axis. Images were filtered to optimize catheter sensor visibility. The following coordinates were labeled on each video frame: 1) anterior-superior corner of each visible sensor; 2) posterior-inferior border of the cricoid cartilage as it intersects the trachea; and 3) anterior tubercle of C1 vertebra. The posterior-inferior border of the cricoid cartilage corresponded to the position of the CP as it attaches to the cricoid<sup>7,9,19</sup>. The anterior tubercle of C1 represented a stable reference point and was set as the origin of the x- and y-axes. Timing was normalized to the first frame of deglutitive anterior hyoid movement. UES high-pressure zone boundaries were defined according to the span of elevated resting pressure on the manometric plot (Figure 1)<sup>7</sup>. All movement measurements were converted from pixels to cm with the manometric sensor housing (4mm) as a scalar. At each video frame, the UES was assigned a range of HRM sensors according to its position adjacent to the catheter. The combined data set was used to identify deglutitive UES pressure patterns during its elevation.

HRM data were analyzed using a customized Matlab program (The MathWorks, Inc., Natick, MA). For this analysis, we focused on the pressure signal that is measurable after the peak clearance force occurs in the pharynx and UES. The rate of pressure release was calculated by averaging first derivatives from the point that the signal first decreased from maximum pressure until the signal returned to baseline pressure. Thus, a rounded pressure wave would have a slower release rate than a pressure wave with a sharp drop-off. Pressure duration was calculated from the first point that the pressure signal rose from baseline until the point that the pressure signal returned to baseline. Videofluoroscopic and HRM data were analyzed by different research-team members.

Paired t-tests were used for all comparisons with a Bonferroni-corrected  $\alpha$  of  $0.05/11=0.0045$  to determine significance. Effect size was calculated using Cohen's  $d$ , with 0.8 indicating a large effect size<sup>27</sup>. Twenty percent of videofluoroscopic data were reanalyzed by a separate research team member, and intraclass correlation coefficients (ICC) were calculated for reliability. Data are reported as mean  $\pm$  standard error.

## RESULTS

**Manometric Sensor and UES Movement**—Due to velopharyngeal-port closure, all sensors at and below the level of the soft palate are drawn superiorly with palate elevation and return to baseline with palatal muscle relaxation. The UES elevates with hyolaryngeal excursion and descends following the bolus tail. See Figure 2 for an example of manometric sensor and UES movement patterns during a swallow. The UES high-pressure zone moves asynchronously from the manometric sensors. Sub-atmospheric pressures occur at the maximum time-point of UES elevation, and contact-pressure are registered as the UES begins to descend.

Figure 3 displays averaged relative movement time-points and durations of the manometric sensors and UES, along with onset of velopharyngeal pressure and UES opening and closure times. Sensors rose significantly before the onset of pressure in the nasopharynx ( $0.15 \pm 0.12$  seconds;  $t(10)=4.2$ ,  $p=0.002$ ; Cohen's  $d=1.27$ ). Sensors moved significantly before the UES when rising from baseline ( $0.09 \pm 0.02$  seconds;  $t(10)=5.99$ ,  $p<0.001$ ; Cohen's  $d=1.80$ ) and when falling from maximal rise ( $0.29 \pm 0.04$  seconds;  $t(10)=6.67$ ,  $p<0.001$ ; Cohen's  $d=2.01$ ). Sensors returned to baseline position before the UES returned to baseline position, but this difference did not reach significance according to our  $\alpha$ -criterion ( $0.20 \pm 0.04$  seconds;  $t(10)=4.94$ ,  $p=0.01$ ; Cohen's  $d=1.49$ ). Although not temporally-aligned, there was no significant difference in duration of rise over baseline position between the sensors ( $1.25 \pm 0.10$  seconds) and UES ( $1.21 \pm 0.09$  seconds;  $t(10)=1.32$ ,  $p=0.22$ , Cohen's  $d=0.6721$ ).

Movement amplitudes are in Table 1. The anterior aspect of the UES, recorded at its cricoid attachment, moved to a significantly greater extent in both ventral ( $t(10)=4.538$ ,  $p=0.01$ ; Cohen's  $d=1.37$ ) and rostral directions ( $t(10)=10.84$ ,  $p<0.001$ ; Cohen's  $d=3.27$ ) compared to manometric sensor movements. ICC values for sensor and UES position identification ranged from 0.90–0.97, indicating strong intra-rater agreement.

**Manometric UES Waveform Analysis**—Due to the movements of the manometric catheter and UES, UES pressure registers on 4–6 manometric sensors during a swallow. We discerned two distinct pressure patterns from these sensors: 1) Caudal-UES pattern: elevated pressure at baseline, fall to nadir pressure, pressure burst, and return to baseline pressure from the most caudal 2–3 sensors; and 2) Rostral-UES pattern: a relatively brief pressure wave with a fast rate of pressure release from 1–3 sensors directly rostral to the caudal-UES pattern. Representative individual pressure waveforms are displayed in Figure 4. Rostral-UES pressure signals had significantly faster rates of pressure release ( $-0.0989 \pm 0.0143\text{mmHg/seconds}^2$ ) versus both caudal-UES pressure signals ( $-0.0073 \pm 0.0008\text{mmHg/seconds}^2$ ;  $t(10)=6.44$ ,  $p<0.001$ , Cohen's  $d=1.94$ ) and other pharyngeal pressure signals ( $-0.0374 \pm 0.0023\text{mmHg/seconds}^2$ ;  $t(10)=4.14$ ,  $p=0.002$ , Cohen's  $d=1.24$ ). Duration of pressure above baseline was significantly shorter for rostral-UES pressure signals ( $0.39 \pm 0.21$  seconds) versus any other pharyngeal pressure signal ( $0.62 \pm 0.10$  seconds;  $t(10)=5.95$ ,  $p<0.001$ , Cohen's  $d=1.79$ ).

## STUDY 2: HRM+EMG

### Equipment

High-Resolution Manometry: Specifications of the manometric system and procedures for catheter placement are the same as Study 1.

Electromyography: Cricopharyngeal-electromyography (CP-EMG) signals were recorded with a bipolar, hook-wire, intramuscular electrode (50 $\mu$ m diameter; MicroProbes, Gaithersburg, MD) and submental/suprahoid muscle group activity was recorded with bilateral surface-EMG electrodes on the submental region, placed 1cm from midline. A surface ground electrode (A10058-SRT; Vermed, Bellows Falls, VT) was secured on the forehead. EMG signals were amplified, bandpass-filtered from 100 Hz to 6 kHz<sup>28</sup> (model 15LT; Grass Technologies, Warwick, RI) and digitized at 20 kHz (LabChart version 6.1.3; ADInstruments, Colorado Springs, CO). EMG data were time-linked to manometry data via a common computer mouse creating logic signals upon the manometric and EMG signals.

### Participants

Six adults (4 males) participated with informed consent and under approval from the University of Wisconsin-Madison Institutional Review Board. Participants were of a mean age of 22.7 years (range: 21–25) and had no history of swallowing, gastrointestinal, or neurologic disorders. These participants did not overlap with those in Study 1.

### Procedure

One mL of 1% lidocaine hydrochloride with epinephrine (1:100,000) was injected into the neck with a 30-gauge needle prior to electrode insertion. The intramuscular electrode was placed into the CP with a 27-gauge needle. Once characteristic deglutitive CP activation patterns were identified<sup>6</sup>, the needle was removed, leaving the electrode in place. Accurate placement of the CP-EMG electrode was confirmed by visualization of characteristic CP-EMG activity. The necessary CP-EMG parameters include tonic baseline activity, decrease to nearly zero, a post-swallow burst of activity with a rapid onset, and return to baseline activity<sup>6</sup>. Participants swallowed five 10mL boluses of room-temperature water with the head in a neutral position. Participants waited to swallow until cued by the experimenter.

### Data Analysis

HRM and EMG data were analyzed using customized Matlab programs. The CP-EMG signals were re-sampled to 50 Hz to match HRM sampling rate. HRM sensors that matched the deglutitive rostral-UES and caudal-UES pressure patterns described in Study 1 were included in Study 2 analysis. Due to CP-activity quiescence and UES pressure decrease during UES relaxation, there is little activity or pressure from which to calculate associations. Thus, it is difficult, if not impossible, to measure pressure-activity associations as the UES opens. Accordingly, only post-nadir events were examined. The post-nadir UES contractile event is the time-point during swallowing when the most-superior UES pressure signal begins to rise from nadir pressure to the time when the closure CP-EMG activity returns to baseline<sup>28</sup>.



To examine associations between deglutitive UES pressure and CP-EMG activity, we calculated Pearson product-moment correlation coefficients for each trial. As done previously<sup>28</sup>, we calculated correlations over the post-nadir UES contractile event and identified the single manometric sensor with the strongest correlation. Results from Study 1 suggest that post-nadir UES pressure involves multiple sensors, so it is more ecologically-valid to calculate correlation over multiple sensors. Thus, we calculated the Pearson product-moment correlation coefficients between CP-EMG activity and UES pressure in a stepwise, multi-sensor fashion: 1) we first calculated correlation between CP-EMG activity and the most-superior UES sensor (UES1) starting from its rise from nadir until its peak; 2) we then calculated correlation between CP-EMG and the next-inferior sensor (UES2) from the time-point after the peak of UES1 until the peak of UES2; 3) we continued accordingly through all UES sensors (e.g., UES3-5; see Figure 5). We calculated the mean of the multi-sensor correlations for comparison to single-sensor correlation.

To match our directional hypothesis that multi-sensor correlation would be greater than single-sensor correlation, we performed a one-sided, paired-samples t-test to compare single-sensor and multi-sensor correlations, with an  $\alpha$ -criterion of 0.05 to determine significance. Effect size was calculated as in Study 1. Data are reported as mean  $\pm$  standard error.

## RESULTS

As seen in Figure 5, EMG activity maps closely onto UES pressure. Slightly before UES pressure-drop, CP-EMG activity decreases. As EMG activity returns following UES-opening, UES pressure also rises. High levels of EMG activity following quiescence gradually return to baseline activity levels at a similar rate as the UES pressure. Multi-sensor correlation ( $0.88 \pm 0.04$ ) was significantly stronger than single-sensor correlation ( $0.80 \pm 0.04$ ;  $t(5)=2.95$ ,  $p=0.02$ ; Cohen's  $d=1.20$ ). The improved correlation using multiple sensors supports the assumption that during bolus transport, the UES has risen such that its closure pressures influence as many as 6 different sensors during descent to its baseline location.

## DISCUSSION

Rostral-UES movement during deglutitive relaxation and contraction creates pressure patterns on HRM that are mathematically-distinct from other pressure patterns in the pharyngo-esophagus. CP-EMG activity has stronger correlations with multi-sensor UES pressure patterns than with a single sensor. To our knowledge, this is the first study describing rostral-UES and caudal-UES pressures on high-resolution manometry, with distinct patterns that can be visually identified without complex mathematics or additional instrumentation, such as videofluoroscopy.

Study 1 confirms previous conventional manometry findings<sup>7,19</sup>. The manometric catheter moves asynchronously and to a lesser-degree than the UES. This suggests different physiologic mechanisms are responsible for each: velopharyngeal-port closure moves the catheter rostrally, and hyolaryngeal excursion with pharyngeal shortening result in UES elevation. Previous descriptions of manometric catheter movement did not evaluate pressure

generated by velopharyngeal-port closure<sup>7,19</sup>. While catheter movement was temporally-related to velopharyngeal port closure, the manometric sensors started rostral movement ~0.15 seconds before pressure in the velopharynx registered on HRM. This likely reflects time needed for velopharyngeal musculature to make measurable contact with the sensor and posterior pharyngeal wall, as initial catheter elevation will occur prior to a fully-closed velopharynx<sup>29,30</sup>. Thus, when evaluating HRM without videofluoroscopy, it may be assumed that the catheter has ascended when velopharyngeal pressure initiates.

Ventral movement of manometric sensors has not been previously described. A potential cause may be deglutitive anterior-bulging of the pharyngeal constrictors at the bolus tail. The ventral movements were small and perpendicular to bolus flow, with unknown relevance to interpretation of normal-swallowing physiology.

Currently, otolaryngologists, gastroenterologists, and speech-language pathologists perform HRM at over 250 institutions worldwide<sup>17,18</sup>. With growing clinical and research adoption of HRM, a consistent, clinically-appropriate, and computationally-simple method for identifying deglutitive UES pressures is needed. With results from the present studies, we propose two classifications of UES pressure patterns seen on HRM: rostral-UES and caudal-UES. Rostral-UES pressure patterns are significantly shorter in duration and display a faster rate of pressure release than any other deglutitive pressure pattern in the pharynx. The fast pressure release at these sensors suggests the UES closes against the catheter as it descends, following the bolus tail. Caudal-UES pressure patterns have been well-described: elevated baseline pressure, pressure drop to nadir, a closing burst of pressure, and gradual decline to baseline pressure<sup>2,16,31</sup>. These caudal-UES sensors reside within the UES high-pressure zone at both the beginning and end of the swallow, but may be situated in the proximal esophagus during bolus transit due to UES elevation. Multiple HRM sensors are needed to describe UES pressures. Using a single sensor for analysis potentially misses critical pressure amplitude and timing information, and collapsing data into one signal using eSleeve functionality has not been validated in the UES. This identification of rostral-UES and caudal-UES pressure patterns enables identification of UES location without use of videofluoroscopy or EMG.

The present findings hold important implications for clinical and research interpretations of UES pressures. First, timing of UES opening and closure should be measured with consideration that UES rise is asynchronous to HRM sensor rise and that the UES starts contracting as it is still above its baseline position. Thus, it is likely that the pressure nadir on the most caudal UES sensor (e.g., Sensor 12 in Figures 1, 2, and 4) reflects UES rise and not relaxation. Secondly, post-nadir pressure increase on this same sensor likely reflects UES descent and not closure. We recommend measuring the timing of UES closure as the time when the most rostral sensor with the rostral-UES pressure pattern (e.g., Sensor 8 in Figures 1, 2, and 4) rises from relaxation pressure. Finally, the ideal location at which to measure UES nadir pressure remains unclear. In Figure 2, it is evident that the UES is situated over Sensors 8, 9, and 10 during relaxation and that Sensors 11 and 12 are located in the rostral esophagus at this point. It follows that the UES nadir pressure should be measured over Sensors 8, 9, and 10 during this swallow. However, the physiologic relevance of esophageal sub-atmospheric pressure on bolus transport<sup>21</sup> remains to be shown. Further



work will inform UES nadir pressure analysis for clinical and research purposes, but we present clear findings that can guide decisions on where to measure UES opening and closure.

Three limitations in these studies should be noted. First, analysis was performed on a modest-sized sample of young, healthy participants. This is an important first step in understanding UES pressure-movement relationships, and future studies will examine how UES patterns observed in this study present in states of dysphagia. Second, analysis of videofluoroscopy was limited to 30 frames/second. Higher-frequency fluoroscopic data acquisition, if possible, may result in stronger pressure-movement relationships. Third, transcutaneous placement of the EMG electrode in the cricopharyngeus without direct visualization posed a unique challenge, resulting in a relatively small number of participants displaying a clear CP-EMG trace. Future studies involving intramuscular CP-EMG would benefit from guided approaches, such as videofluoroscopy or ultrasonography.

## CONCLUSIONS

During swallowing, velopharyngeal port closure causes rostral manometric catheter movement, and the UES moves independently. We described patterns of UES pressure using HRM+videofluoroscopy and HRM+EMG. The caudal-UES pressure pattern has been previously described; it represents the UES at rest before the swallow and UES pressure as it descends to a baseline position following bolus passage. This is the first report of a rostral-UES pattern that has a short duration of pressure with a fast rate of pressure release. This pattern represents closure of the UES at an elevated position and its descent to baseline position. These patterns are correlated with CP-EMG and are identifiable without the use of other assessment modalities or complex mathematics. In order to fully capture deglutitive UES pressure, one must evaluate multiple, closely-spaced manometric sensors. The pressure patterns revealed as part of this study will allow researchers and clinicians to locate the UES with only use of HRM.

## ACKNOWLEDGEMENTS

This work was supported by National Institutes of Health grants DC011130, DC010900, T32 GM007507 and RR025012 and an internal grant from the Department of Surgery at the University of Wisconsin-Madison. The authors acknowledge Glen Levenson, PhD, biostatistician, for his assistance with statistical analysis and Matthew Hoffman, PhD, Chelsea Walczak, BS, Levi Brown, and Alyssa Mitchell for their assistance with data collection and analysis.

## REFERENCES

1. Asoh R, Goyal RK. Manometry and electromyography of the upper esophageal sphincter in the opossum. *Gastroenterology*. 1978; 74:514–520. [PubMed: 631481]
2. Lang IM, Dantas RO, Cook IJ, Dodds WJ. Videoradiographic, manometric, and electromyographic analysis of canine upper esophageal sphincter. *American Journal of Physiology*. 1991; 260:G911–G919. [PubMed: 2058678]
3. Medda BK, Lang IM, Dodds WJ, et al. Correlation of electrical and contractile activities of the cricopharyngeus muscle in the cat. *The American journal of physiology*. 1997; 273:G470–G479. [PubMed: 9277427]

4. Welch RW, Luckmann K, Ricks PM, Drake ST, Gates GA. Manometry of the normal upper esophageal sphincter and its alterations in laryngectomy. *The Journal of clinical investigation*. 1979; 63:1036–1041. [PubMed: 447825]
5. van Overbeek JJM, Wit HP, Paping RHL, Segenhout HM. Simultaneous manometry and electromyography in the pharyngoesophageal segment. *Laryngoscope*. 1985; 95:582–584. [PubMed: 3990488]
6. Doty RW, Bosma JF. An electromyographic analysis of reflex deglutition. *Journal of neurophysiology*. 1956; 19:44–60. [PubMed: 13286721]
7. Kahrilas PJ, Dodds WJ, Dent J, Logemann JA, Shaker R. Upper esophageal sphincter function during deglutition. *Gastroenterology*. 1988; 95:52–62. [PubMed: 3371625]
8. Cook IJ, Dodds WJ, Dantas RO, et al. Opening mechanisms of the human upper esophageal sphincter. *American Journal of Physiology*. 1989; 257:G748–G759. [PubMed: 2596608]
9. Jacob P, Kahrilas PJ, Logemann JA, Shah V, Ha T. Upper esophageal sphincter opening and modulation during swallowing. *Gastroenterology*. 1989; 97:1469–1478. [PubMed: 2583413]
10. Ghosh SK, Pandolfino JE, Zhang Q, Jarosz A, Kahrilas PJ. Deglutitive upper esophageal sphincter relaxation: a study of 75 volunteer subjects using solid-state high-resolution manometry. *American Journal of Physiology-Gastrointestinal and Liver Physiology*. 2006; 291:G525–G531. [PubMed: 16645162]
11. Nguyen NP, Smith HJ, Moltz CC, et al. Prevalence of Pharyngeal and Esophageal Stenosis following Radiation for Head and Neck Cancer. *J Otolaryngol-Head Neck Surg*. 2008; 37:219–224. [PubMed: 19128616]
12. Munoz AA, Shapiro J, Cuddy LD, Misono S, Bhattacharyya N. Videofluoroscopic findings in dysphagic patients with cricopharyngeal dysfunction: Before and after open cricopharyngeal myotomy. *Ann Otol Rhinol Laryngol*. 2007; 116:49–56. [PubMed: 17305278]
13. Ozgursoy OB, Salassa JR. Manofluorographic and functional outcomes after endoscopic laser cricopharyngeal myotomy for cricopharyngeal bar. *Otolaryngology-Head and Neck Surgery*. 2010; 142:735–740. [PubMed: 20416465]
14. Redmond P, Berliner L, Ambos M, Horowitz L. Radiological assessment of pharyngoesophageal dysfunction with emphasis on cricopharyngeal myotomy. *Am J Gastroenterol*. 1982; 77:85–92. [PubMed: 7072686]
15. Cook I, Dodds W, Dantas R, et al. Timing of videofluoroscopic, manometric events, and bolus transit during the oral and pharyngeal phases of swallowing. *Dysphagia*. 1989; 4:8–15. [PubMed: 2640180]
16. Isberg A, Nilsson ME, Schiratzki H. The upper esophageal sphincter during normal deglutition. A simultaneous cineradiographic and manometric investigation. *Acta radiologica: diagnosis*. 1985; 26:563–568. [PubMed: 4072751]
17. Knigge MA, Thibeault S, McCulloch TM. Implementation of high-resolution manometry in the clinical practice of speech language pathology. *Dysphagia*. 2014; 29:2–16. [PubMed: 24233810]
18. Pandolfino JE. High-resolution manometry: is it better for detecting esophageal disease? *Gastroenterology & Hepatology*. 2010; 6:632–634. [PubMed: 21103442]
19. Isberg A, Nilsson ME, Schiratzki H. Movement of the upper esophageal sphincter and a manometric device during deglutition: A cineradiographic investigation. *Acta Radiologica-Diagnosis*. 1985; 26:381–388. [PubMed: 4050518]
20. Palmer JB, Tanaka E, Ensrud E. Motions of the posterior pharyngeal wall in human swallowing: a quantitative videofluorographic study. *Archives of Physical Medicine and Rehabilitation*. 2000; 81:1520–1526.
21. McConnel FMS. Analysis of pressure generation and bolus transit during pharyngeal swallowing. *Laryngoscope*. 1988; 98:71–78. [PubMed: 3336265]
22. Choi WS, Kim TW, Kim JH, et al. High-resolution Manometry and Globus: Comparison of Globus, Gastroesophageal Reflux Disease and Normal Controls Using High-resolution Manometry. *Journal of neurogastroenterology and motility*. 2013; 19:473–478. [PubMed: 24199007]

23. Kwiatek MA, Mirza F, Kahrilas PJ, Pandolfino JE. Hyperdynamic upper esophageal sphincter pressure: a manometric observation in patients reporting globus sensation. *The American journal of gastroenterology*. 2009; 104:289–298. [PubMed: 19174789]
24. Nicodeme F, Pandolfino JE, Lin Z, Xiao Y, Escobar G, Kahrilas PJ. Adding a radial dimension to the assessment of esophagogastric junction relaxation: validation studies of the 3D-eSleeve. *American Journal of Physiology - Gastrointestinal and Liver Physiology*. 2012; 303:G275–G280. [PubMed: 22628033]
25. Clouse RE, Parks TR, Staiano A, Haroian LR. Creation of an electronic sleeve emulation (eSleeve) for use with solid-state high-resolution manometry (HRM). *Gastroenterology*. 2004; 126:A111–A112.
26. McCulloch TM, Hoffman MR, Ciucci MR. High-resolution manometry of pharyngeal swallow pressure events associated with head turn and chin tuck. *Annals of Otolaryngology, Rhinology, and Laryngology*. 2010; 119:369–376.
27. Cohen, J. *Statistical power analysis for the behavioral sciences*. Hillsdale, NJ: Erlbaum; 1988.
28. Jones CA, Hammer MJ, Hoffman MR, McCulloch TM. Quantifying contributions of the cricopharyngeus to upper esophageal sphincter pressure changes by means of intramuscular electromyography and high-resolution manometry. *Annals of Otolaryngology, Rhinology, and Laryngology*. 2014; 123:174–182.
29. Kendall KA, McKenzie S, Leonard RJ, Goncalves MI, Walker A. Timing of events in normal swallowing: a videofluoroscopic study. *Dysphagia*. 2000; 15:74–83. [PubMed: 10758189]
30. Curtis DJ, Cruess DF, Dachman AH, Maso E. Timing in the normal pharyngeal swallow. Prospective selection and evaluation of 16 normal asymptomatic patients. *Investigative radiology*. 1984; 19:523–529. [PubMed: 6511259]
31. Sokol EM, Heitmann P, Wolf BS, Cohen BR. Simultaneous cineradiographic and manometric study of pharynx, hypopharynx, and cervical esophagus. *Gastroenterology*. 1966; 51:960–&. [PubMed: 5958607]

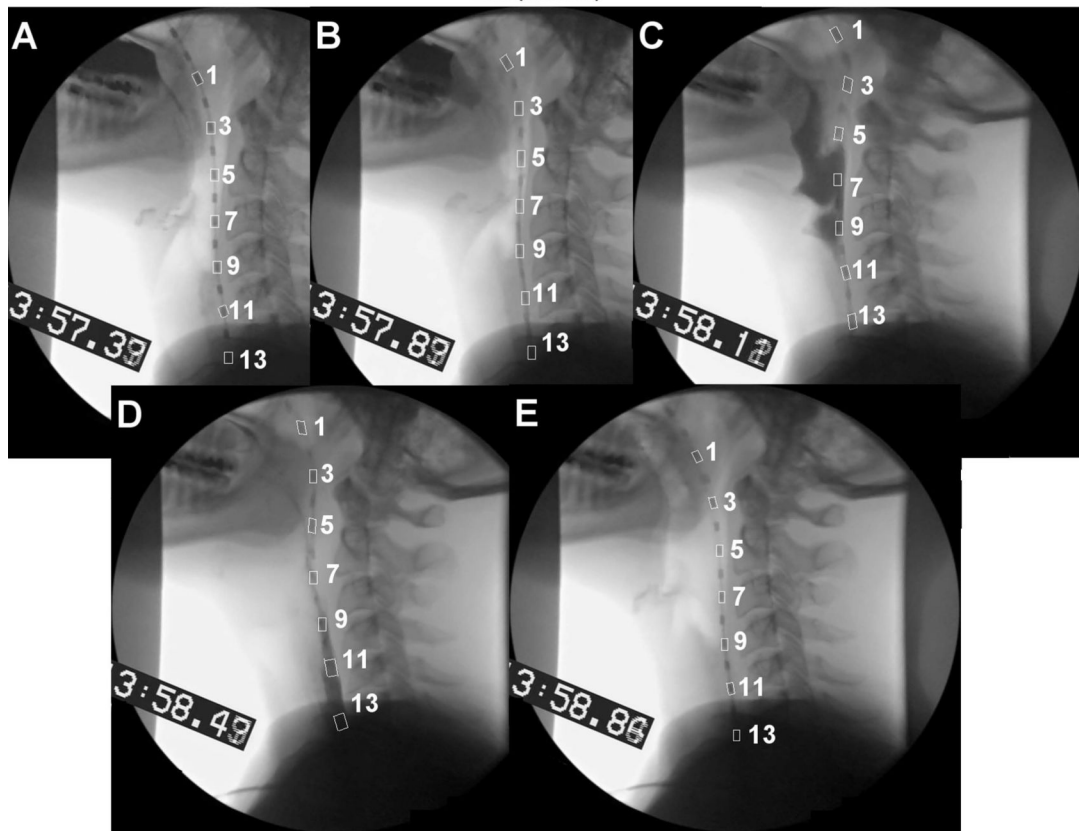
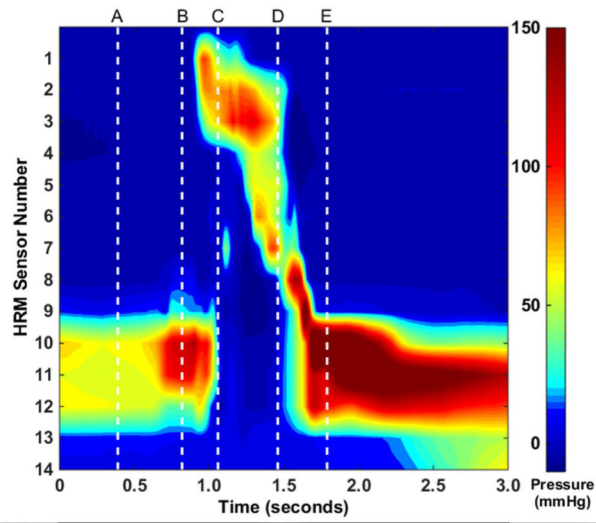


**Figure 1.** High-resolution manometry spatio-temporal plot of a 10 mL thin liquid bolus swallow. The swallow displayed here is the same as those in Figures 2 and 4.

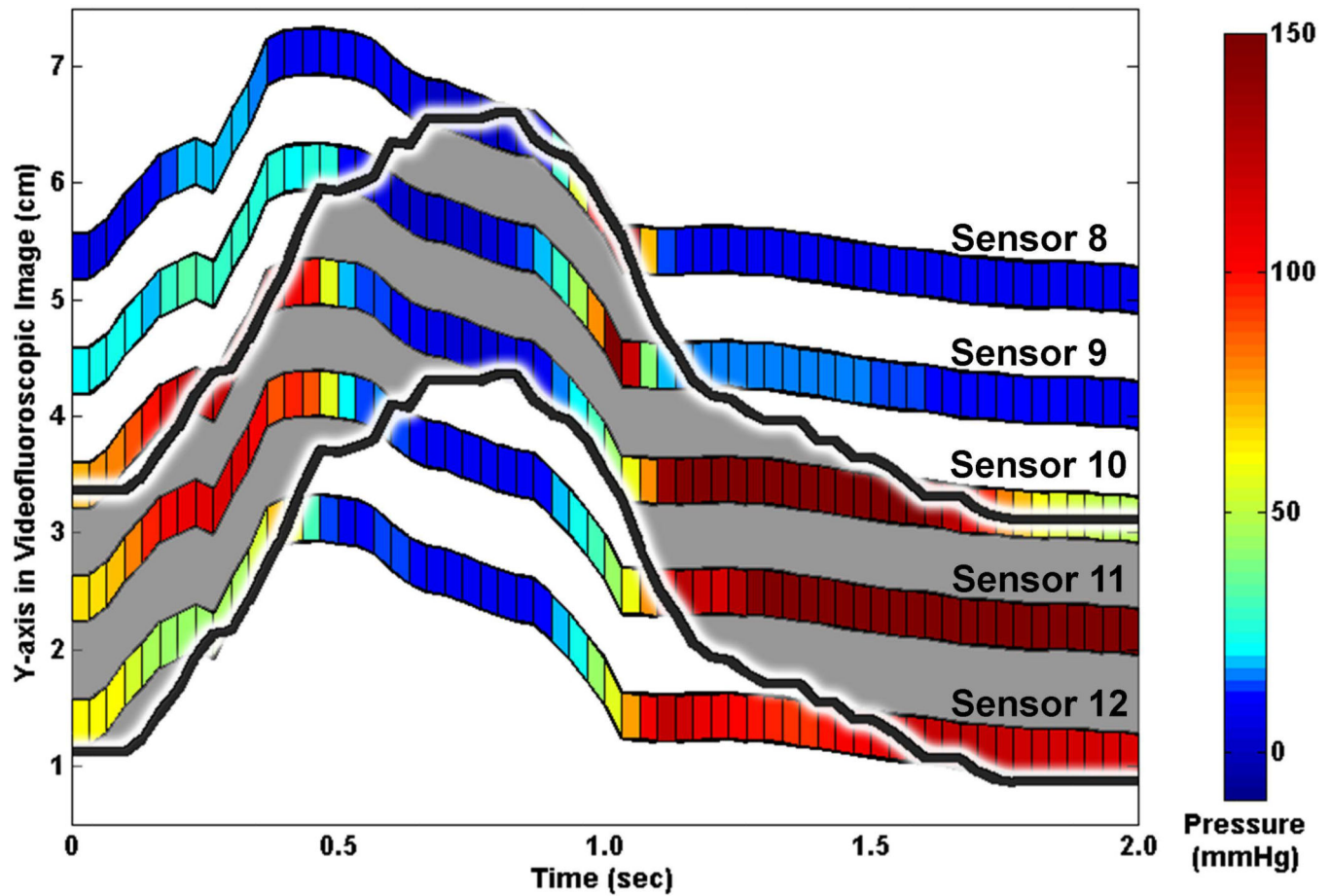


**Figure 2.** Sample plot of manometric sensor and upper esophageal sphincter (UES) deglutitive rostral-caudal movement patterns. Manometric pressure in the UES displayed by colored bars. UES high-pressure zone marked with black line and grey shading. Sensor numbers in this figure correspond to the spatio-temporal plot in Figure 1 and the line plots in Figure 4.

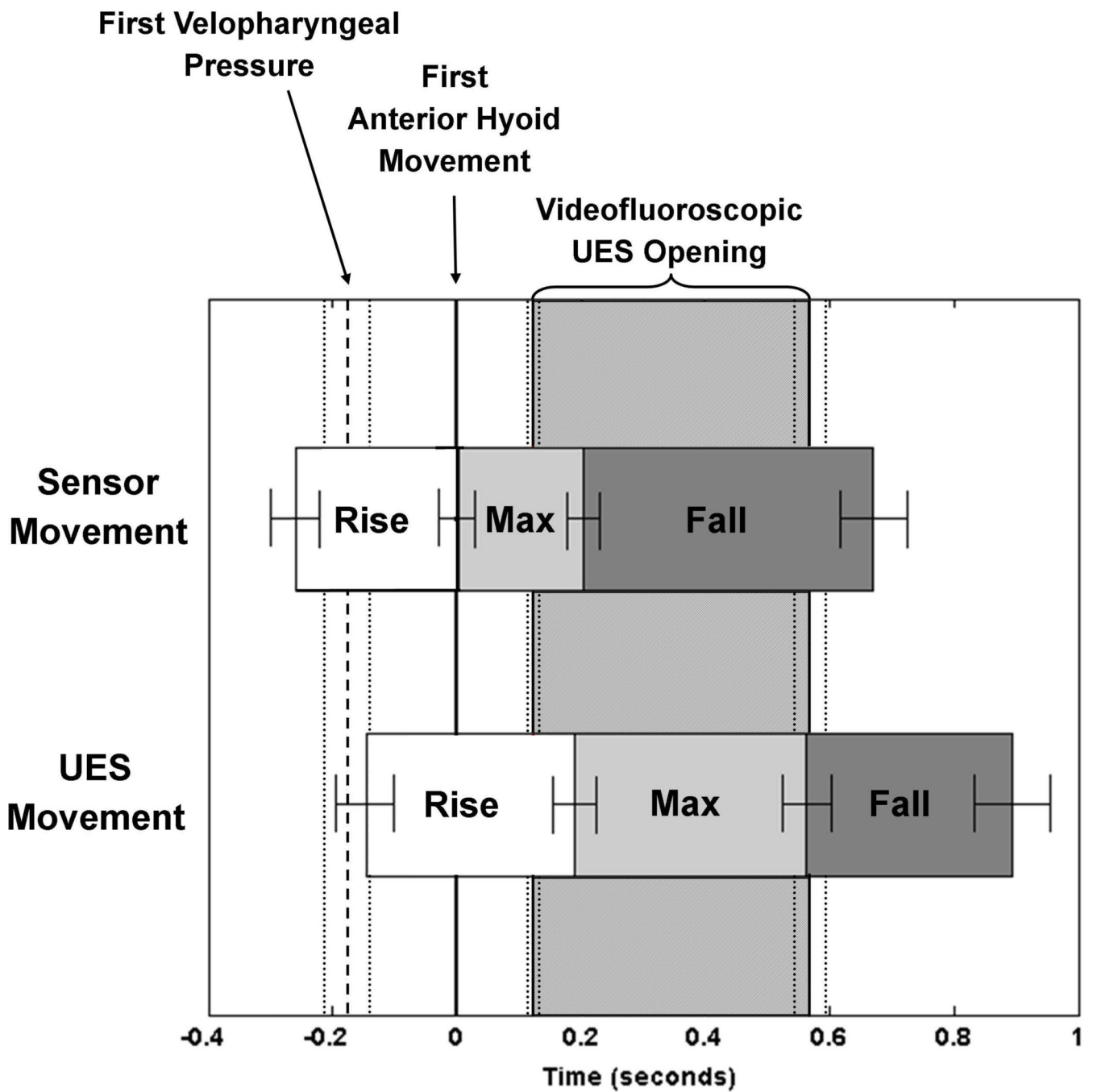


**Figure 3.** Comparison of timing of manometric sensor and upper esophageal sphincter (UES) deglutitive movements in relation to velopharyngeal pressure onset, hyolaryngeal movement, and radiographic UES opening.



**Pharyngeal  
Sensors**

**Rostral UES  
Sensors**

**Caudal UES  
Sensors**

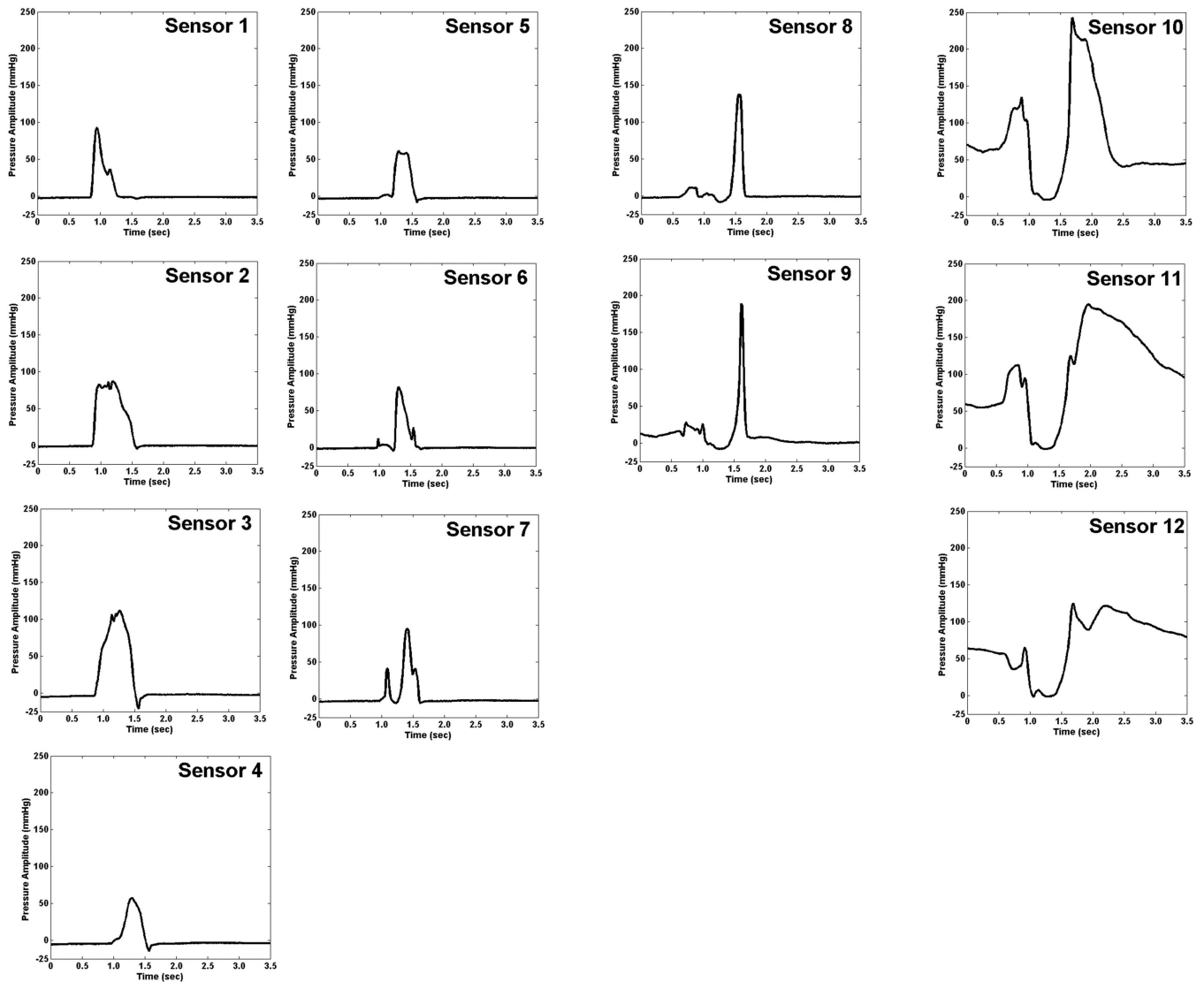


**Figure 4.** Pressure waveform plots from a single 10 mL thin liquid bolus swallow, separated into 3 groups: 1) Pharyngeal sensors; 2) Rostral upper esophageal sphincter (UES) sensors; and 3) Caudal-UES sensors. The swallow displayed here is the same as those in Figures 1 and 2. Sensors 8–12 correspond with the colored lines in Figure 2.

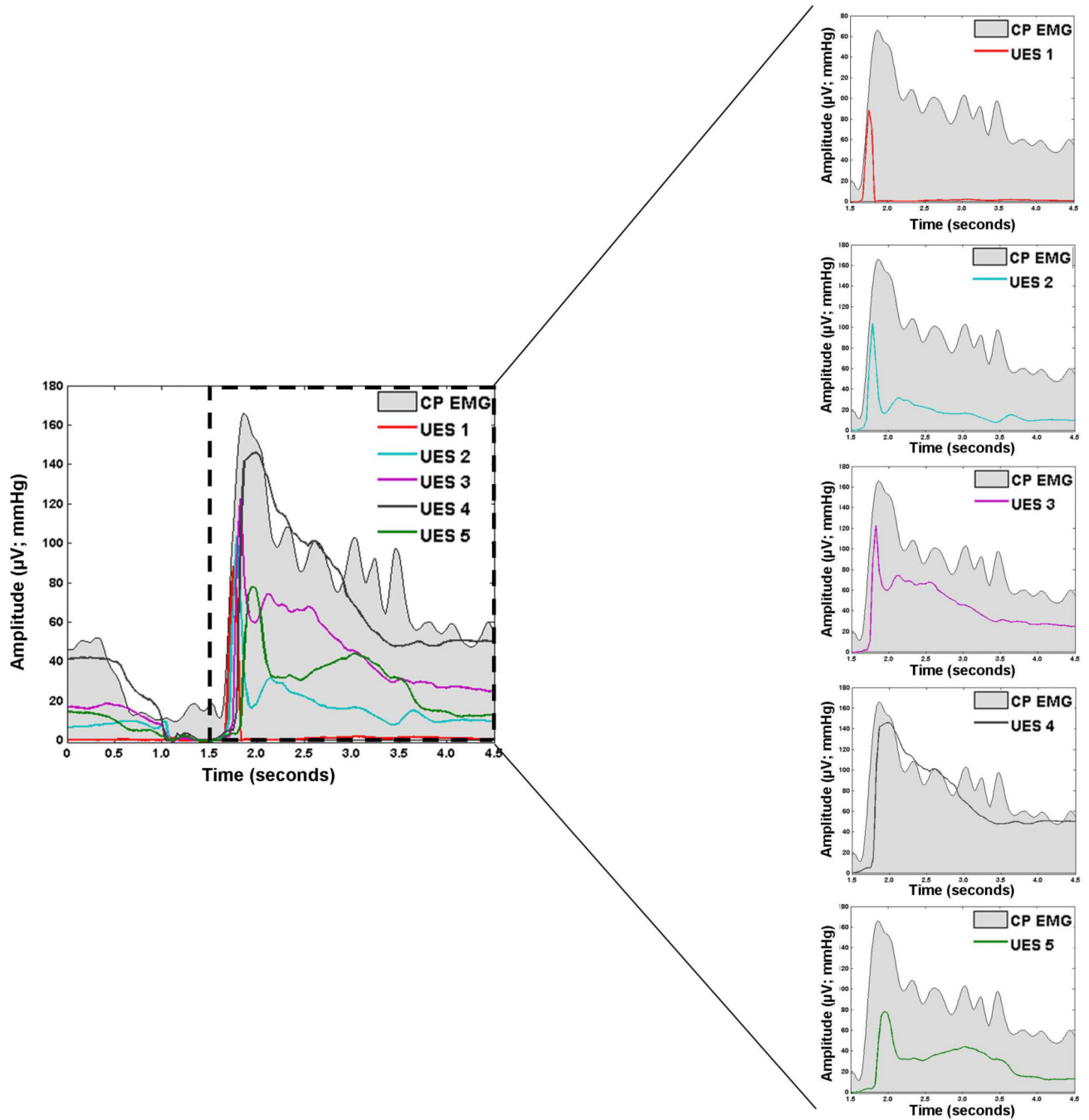


**Figure 5.** Cricopharyngeal electromyography (CP-EMG; grey shading) and upper esophageal sphincter (UES) high-resolution manometry (HRM) pressure waveforms for one 10 mL thin liquid bolus swallow. UES HRM sensors are labeled 1–5 in the rostral to caudal direction.

**Table 1**

Average  $\pm$  standard error of mean values for ventral and rostral movement amplitudes of the manometric sensors and upper esophageal sphincter

	<b>Manometric Sensors</b>	<b>Upper Esophageal Sphincter</b>
Ventral Movement Amplitude (cm)	0.70 $\pm$ 0.07	1.13 $\pm$ 0.10
Rostral Movement Amplitude (cm)	1.21 $\pm$ 0.11	3.10 $\pm$ 0.22

Author Manuscript

Author Manuscript

Author Manuscript

Author Manuscript